

Biophysical Journal, Volume 116

Supplemental Information

**Complex Phase Behavior of GUVs Containing Different
Sphingomyelins**

Daniel Balleza, Andrea Mescola, Nathaly Marín–Medina, Gregorio Ragazzini, Marco Pieruccini, Paolo Facci, and Andrea Alessandrini

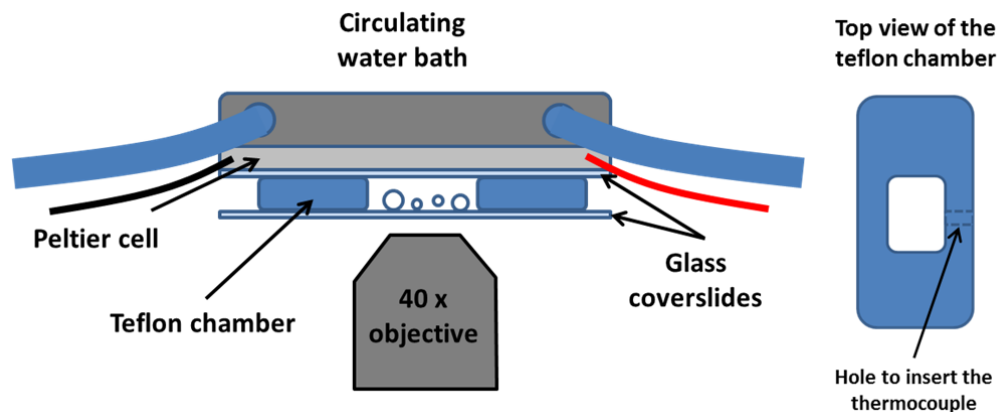


Fig. S1: Scheme of the set-up used to analyze the GUVs at different temperatures with the epifluorescence microscope. The Peltier cell is connected to a home-developed temperature controller device implementing a PID control by the Arduino Uno board. The circulating water bath is exploited as fast heat sink.

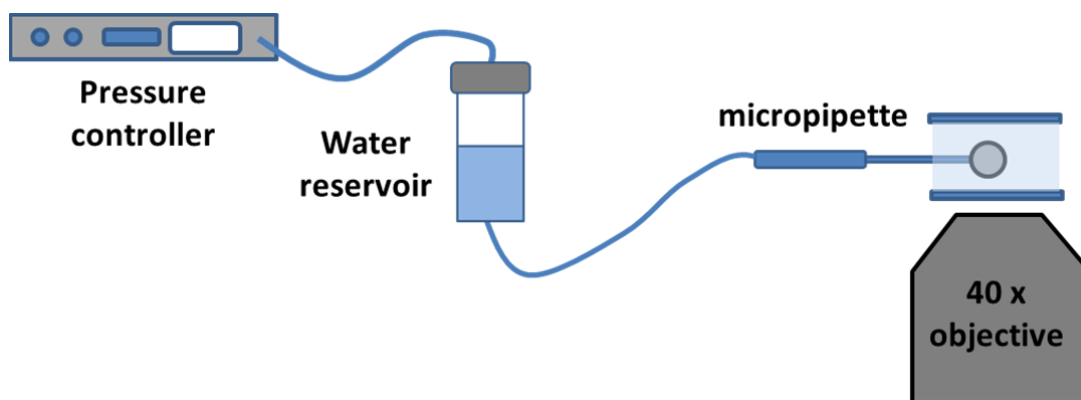


Fig. S2: Scheme of the Micropipette aspiration set-up exploited to change the lateral tension of the GUVs. The pressure controller is used to control the pressure on top of the water reservoir. The water reservoir is connected to the micropipette.

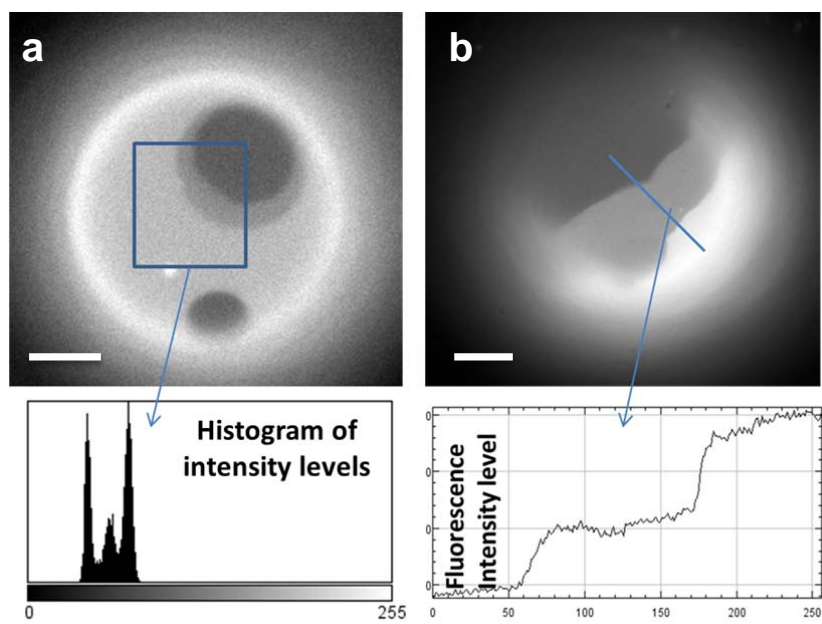


Fig. S3: Fluorescence intensity analysis (histogram of intensity levels in a) and line section in b)) for DiPhyPC/bSM/Cho 1/1/1 GUVs showing three intensity levels. (Bar = 10 μm)

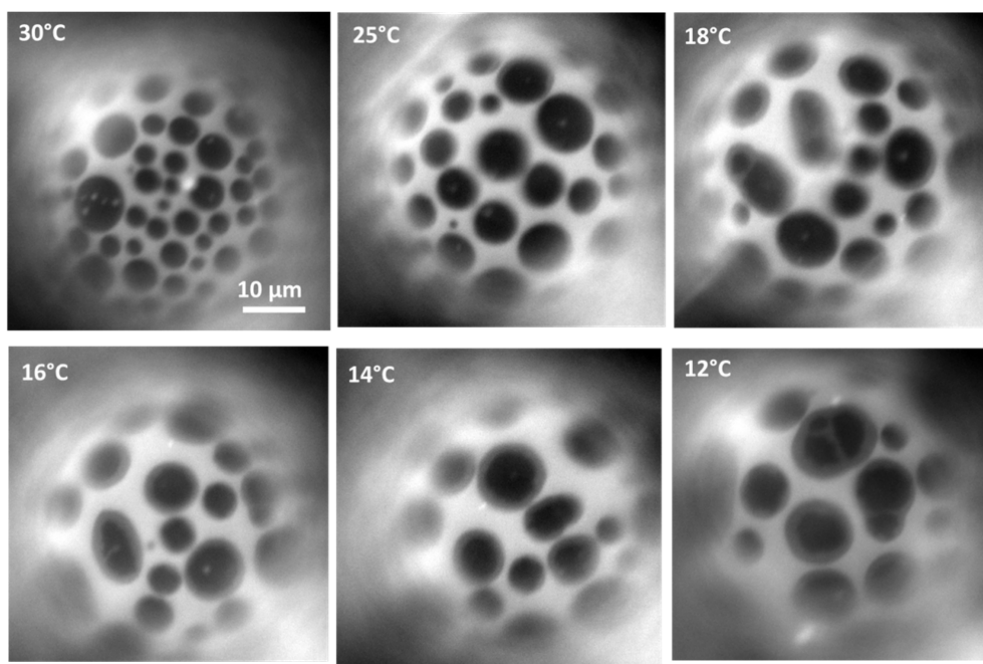
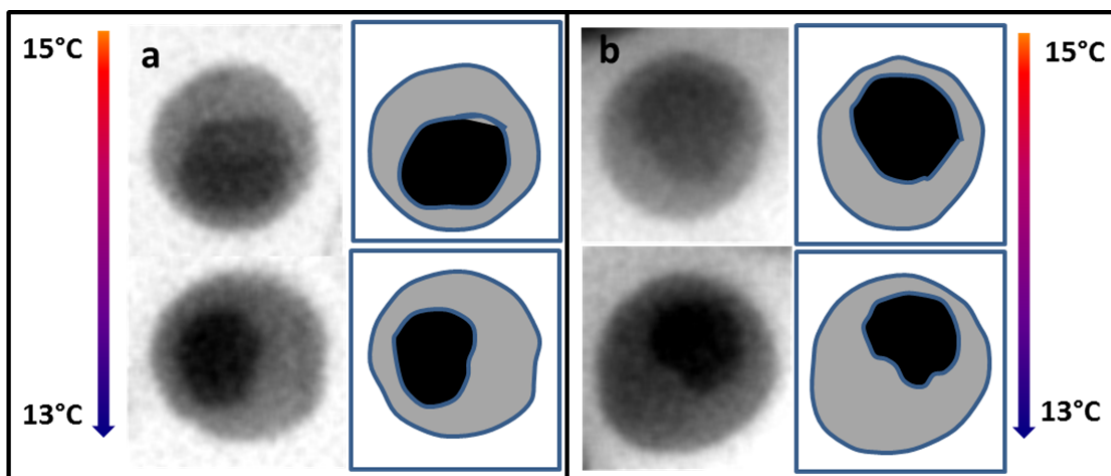


Fig S4: Example of the formation of the intermediate fluorescence intensity level for a DiPhyPC/bSM/Chol 1/1/1 vesicle not grabbed by a micropipette upon a decreasing temperature run.



	15°C		13°C	
	Grey region	Black region	Grey region	Black region
a	79	48	103	39
b	82	51	109	42

Fig. S5: Analysis of the area variation as a function of temperature for the darkest and the intermediate region in the case of two domains (a and b) from the sequence reported in Fig. 2 of the manuscript and Movie S1. Both the fluorescence images and schemes of how the domains have been calculated are reported. The Table reports the area of the different domains for two different temperatures (15°C and 13°C). The grey region is the region defined by the external border of the intermediate fluorescence level whereas the black region is the area of the region with the lowest fluorescence intensity level. The unit for area quantification is μm^2 .

DiPhyPC/bSM/dihydrochol

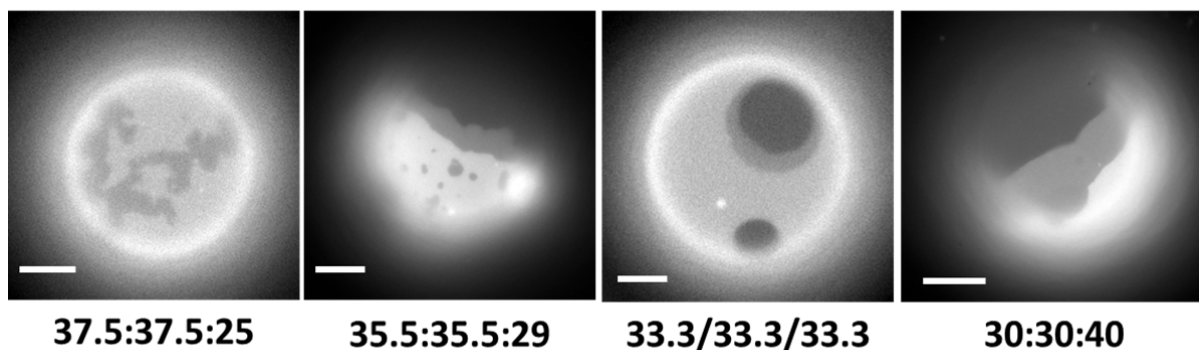


Fig. S6: We considered different molar proportions of the DiPhyPC/bSM/dihydrochol mixture. In particular, keeping an equal molar proportion between DiPhyPC and bSM (1:1) we changed the amount of cholesterol. We found that a low amount of cholesterol ($\sim 25\%$) easily produced the S_o phase coexisting with the L_d phase and the three different fluorescent intensities were never observed. For higher cholesterol concentrations (up to 40%) the coexistence of the three intensities was always observed with no evidence of a dependence of the percentage of GUVs in this state on the cholesterol amount. (Bar = 10 μm)

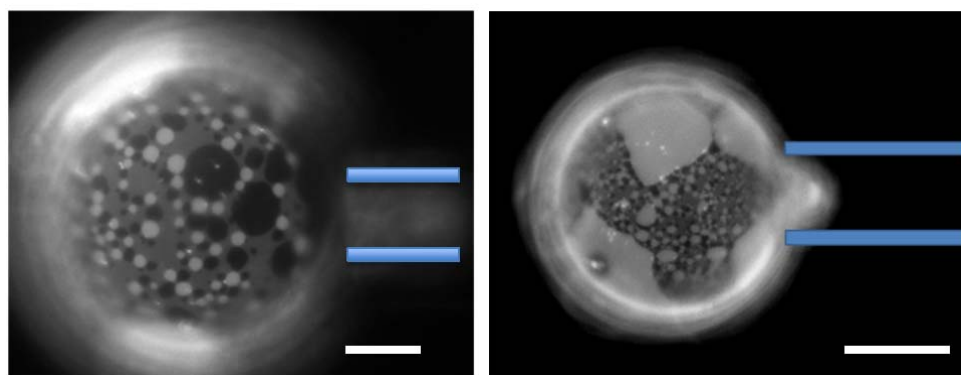


Fig. S7: Examples of other GUVs for which the application of the lateral tension by the MAT set-up induces the appearance in the intermediate fluorescence intensity level region of bright and dark round domains. The blue bars represent the position of the micropipette. (Bar = 10 μm)

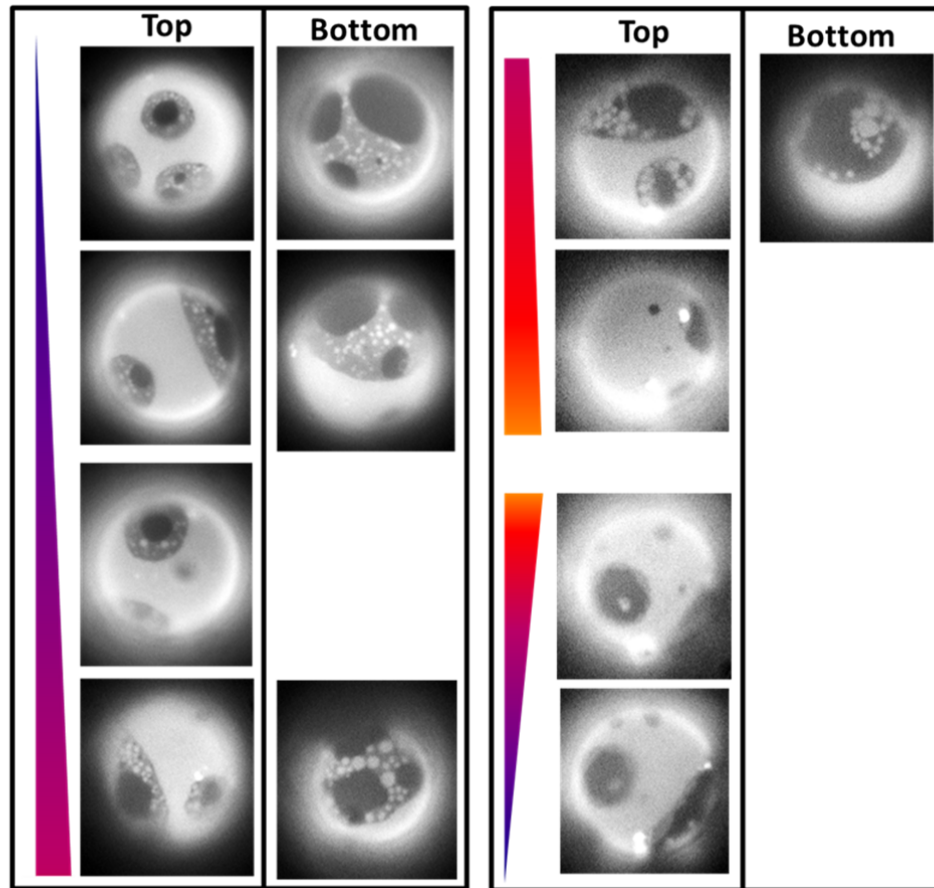


Fig. S8: Sequence of fluorescence microscopy images of a DiPhyPC/bSM/chol 1/1/ 1 GUV (+ 1% Texas Red-DHPE) upon a temperature cycle. The colored triangles and the arrows show the temperature variation trend. Couples of images have been reported when both the top and bottom surfaces of the GUVs have been captured

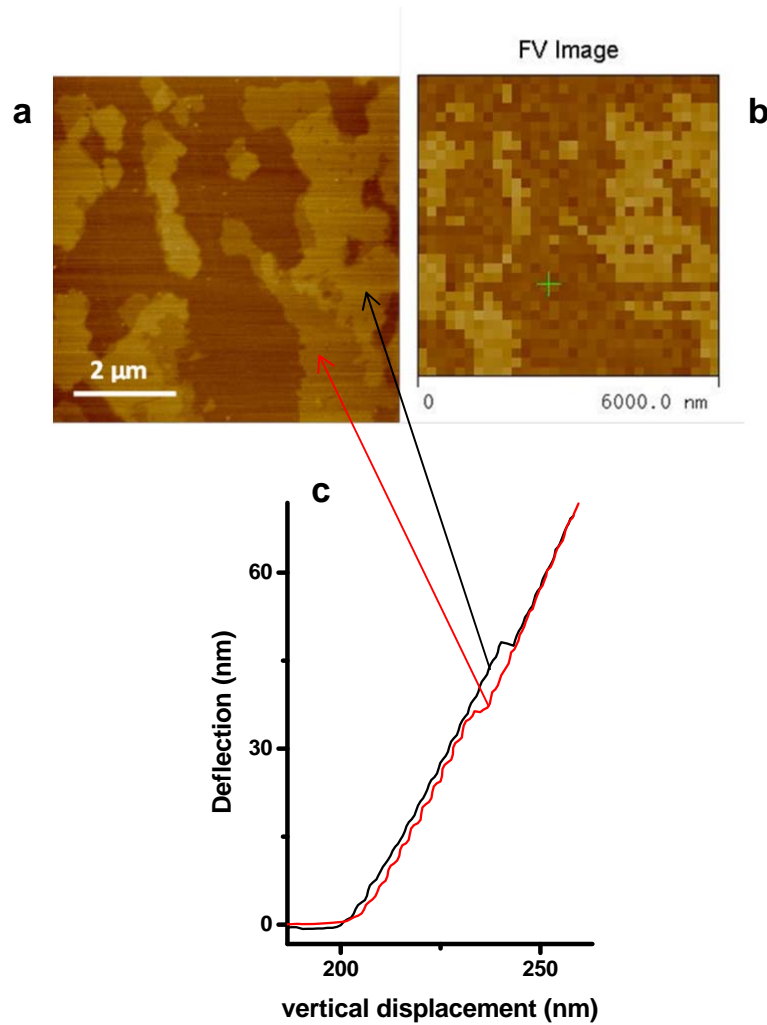


Fig. S9: a) Topography image of a DiPhyPC/bSM/Chol 1/1/1 SLB at 16°C; b) Force Volume image corresponding to the force spectroscopy analysis of the same region in a). The threshold value for the deflection has been chosen to show the punch-through force difference among the different domains; c) two examples of force curves coming from the regions pointed by the arrows.

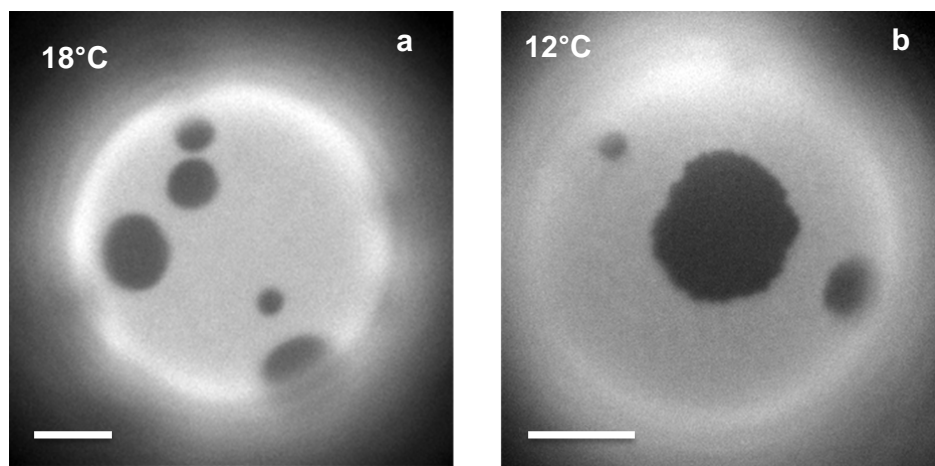


Fig. S10: Examples of fluorescence microscopy images of DiPhyPC/eggSM/chol 1/1/1 (+ 1% Texas Red-DHPE) GUVs. In no cases the presence of more than 2 fluorescence intensity levels has been observed. Bar = 10 μm .

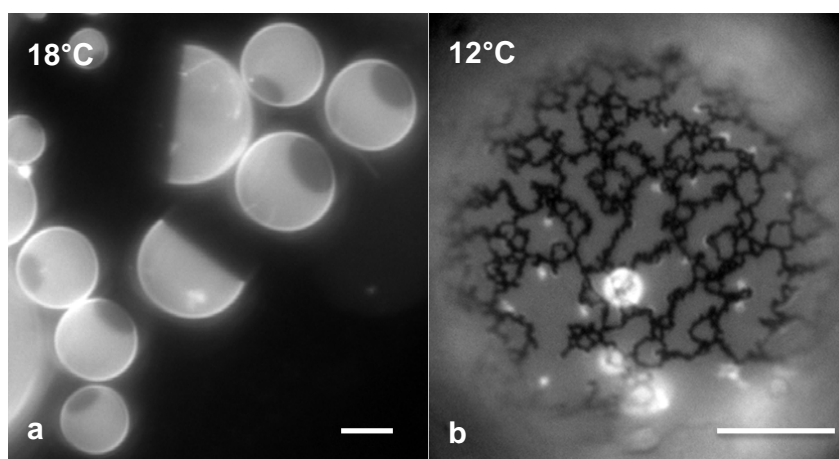


Fig. S11: Examples of fluorescence microscopy images of DiPhyPC/(18:0)SM/Chol 40/40/20 (+ 1% Texas Red-DHPE) GUVs. The presence of more than 2 fluorescence intensity levels has never been observed. Bar = 10 μm .

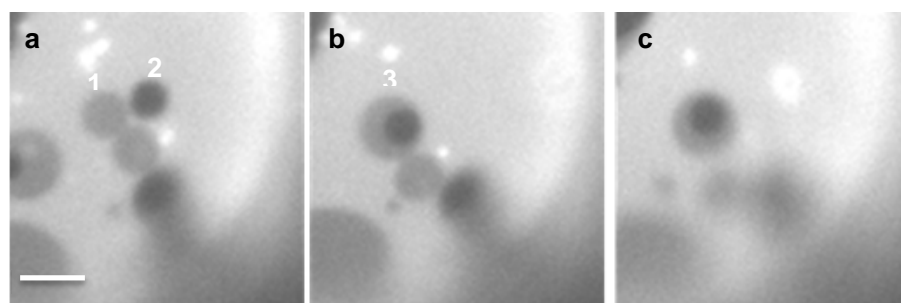


Fig. S12: The sequence shows what happens when a region with the darkest fluorescence intensity merges with an intermediate region. The darkest region is completely included in the intermediate region and the overall area of the domains at the end of the coalescence event is approximately equal to the sum of the two initially separated regions. This behavior is not in accordance with the confinement of the two different domains to the two opposite leaflets. Quantitative analysis of the area of different domains upon coalescence: The area (in pixel²) of domain 1 in a) is 168, for domain 2 we have 102. Upon merging of the two domains, the overall area of the formed domain (3) is 298. The fact that the area of the new domain is almost equal to the sum of the two initial domains points to the fact that the two domains span the overall bilayer thickness and they are not confined to a single leaflet. (Bar = 10 μm)

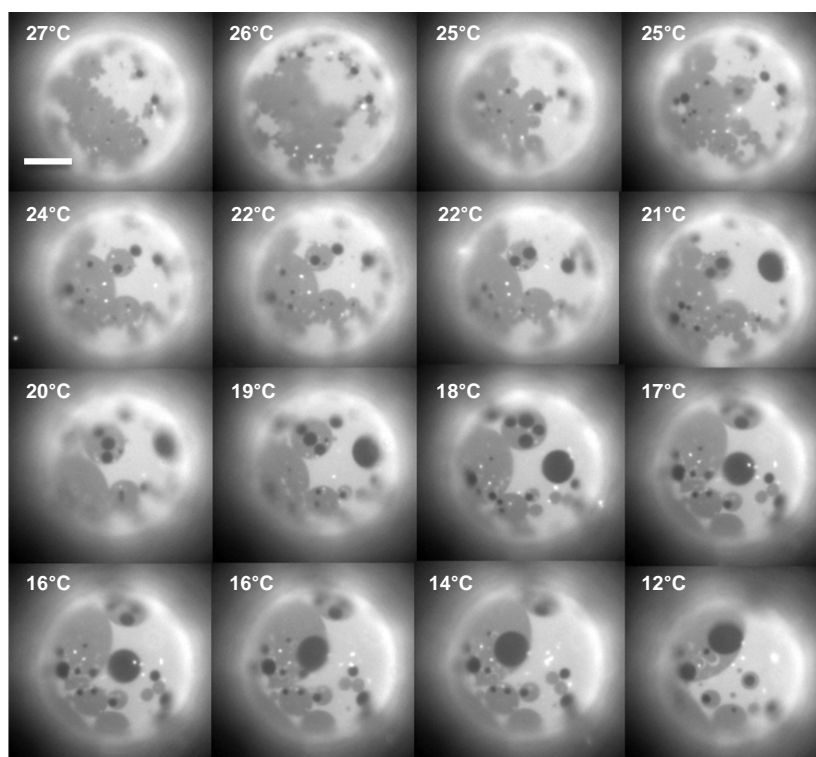


Fig. S13: Sequence of fluorescence microscopy images of a DiPhyPC/(24:1) SM/Chol + 0.5% DHPE Texas Red GUV as the temperature is decreased from 27°C to 12°C. The border between the brightest and the intermediate fluorescence intensity regions gradually gets more defined and regular and the darkest domains, once included inside a larger intermediate domain, get trapped in that position. The sequence corresponds to the vesicle shown in Fig. 7 of the manuscript. (Bar = 10 μm)

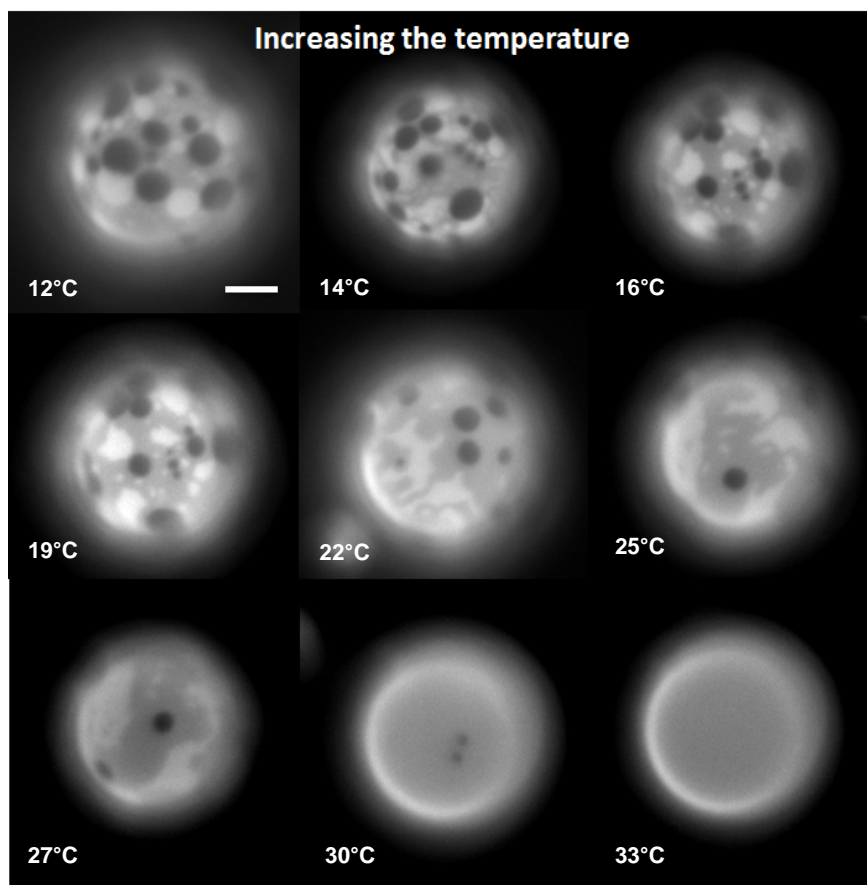


Fig. S14: Phase behavior of a DiPhyPC/(24:1)SM/Chol 1/1/1 (+ 0.5% Texas Red-DHPE) upon temperature increase. Bar = 10 μm .

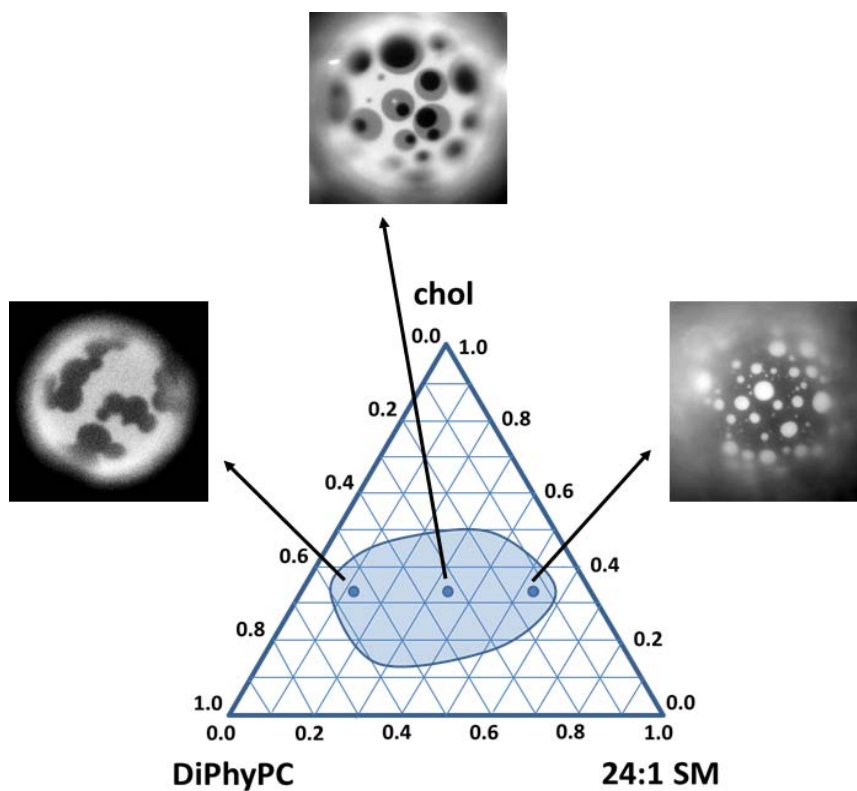


Fig. S15: Appearance of the different fluorescence intensity levels as a function of composition for the ternary mixture DiPhyPC/24:1 SM/chol + 1% Texas Red. The highest fraction of vesicles presenting three fluorescence intensity levels is obtained for a lipid composition with an approximately equal concentration of DiPhyPC and (24:1)SM.

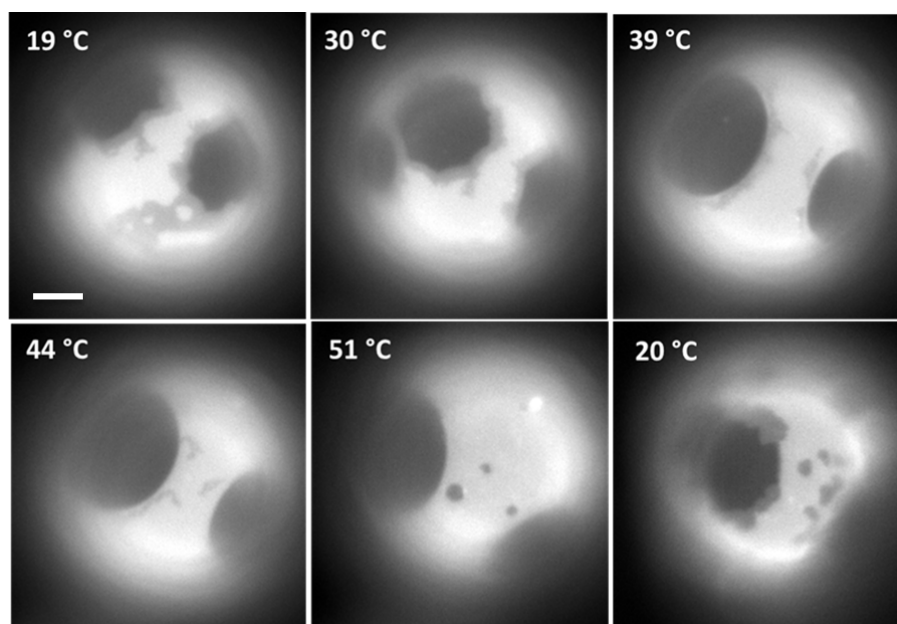


Fig. S16: Sequence of fluorescence microscopy images of a GUV composed by DiPhyPC/(24:0)SM/Chol 1/1/1 plus 1 % DHPE Texas Red. The vesicle has been exposed to a temperature cycle: from 19°C to 51°C and back. The presence of an intermediate fluorescence intensity level wetting the darkest domains is removed at 51°C and reappears at around 25°C. Bar = 10 μ m.

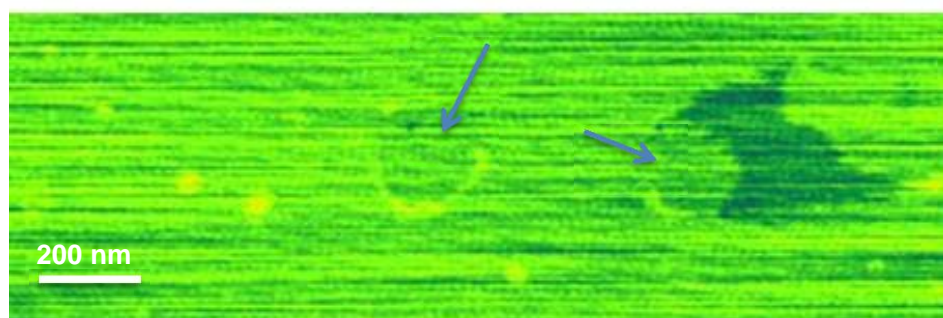


Fig. S17: Higher magnification of Fig. 8a with false colors to highlight the fact that the regions inside the arcs (arrows) have a different height (higher) with respect to the surrounding bilayer. In the false colors representation darkest regions are thicker.

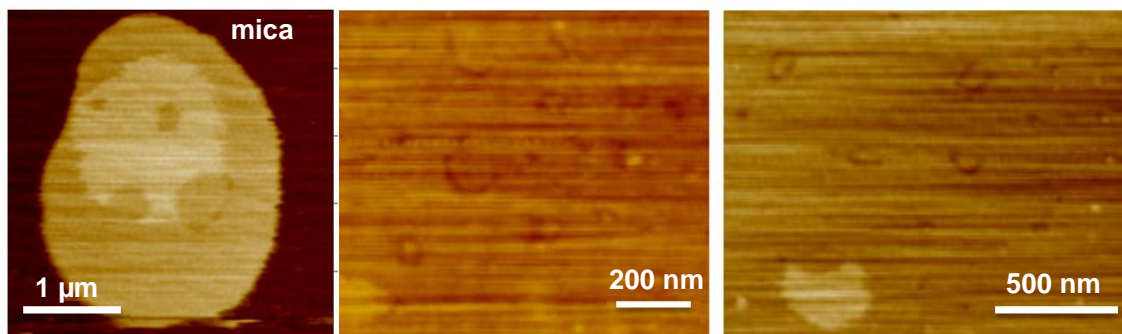


Fig. S18: AFM images of DiPhyPC/(24:1)SM/Chol 1/1/1 SLBs showing the presence of more than two height levels corresponding to the presence of more than two different domain thicknesses. The images have been acquired at a temperature of 12°C

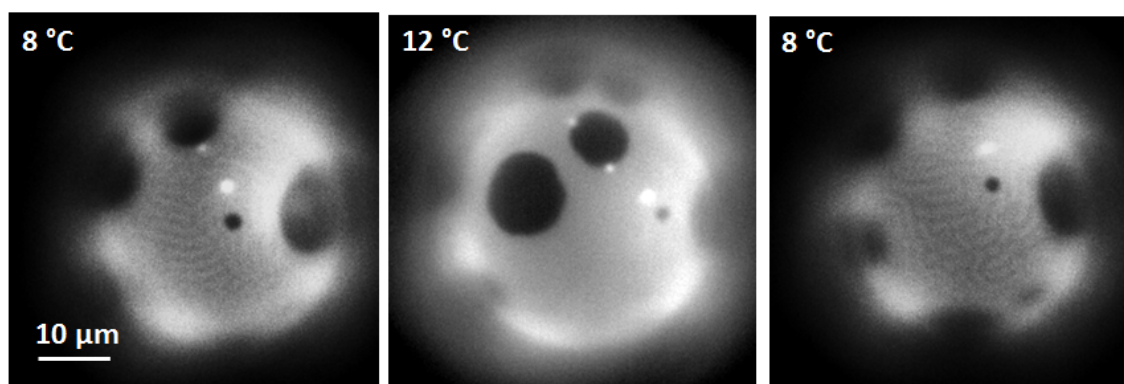


Fig. S19: Appearance of a modulated phase as a function of temperature for a DiPhyPC/(24:1)SM/Chol 1/1/1 +1% Texas Red DHPE GUV. The appearance and disappearance of the modulation is reversible.

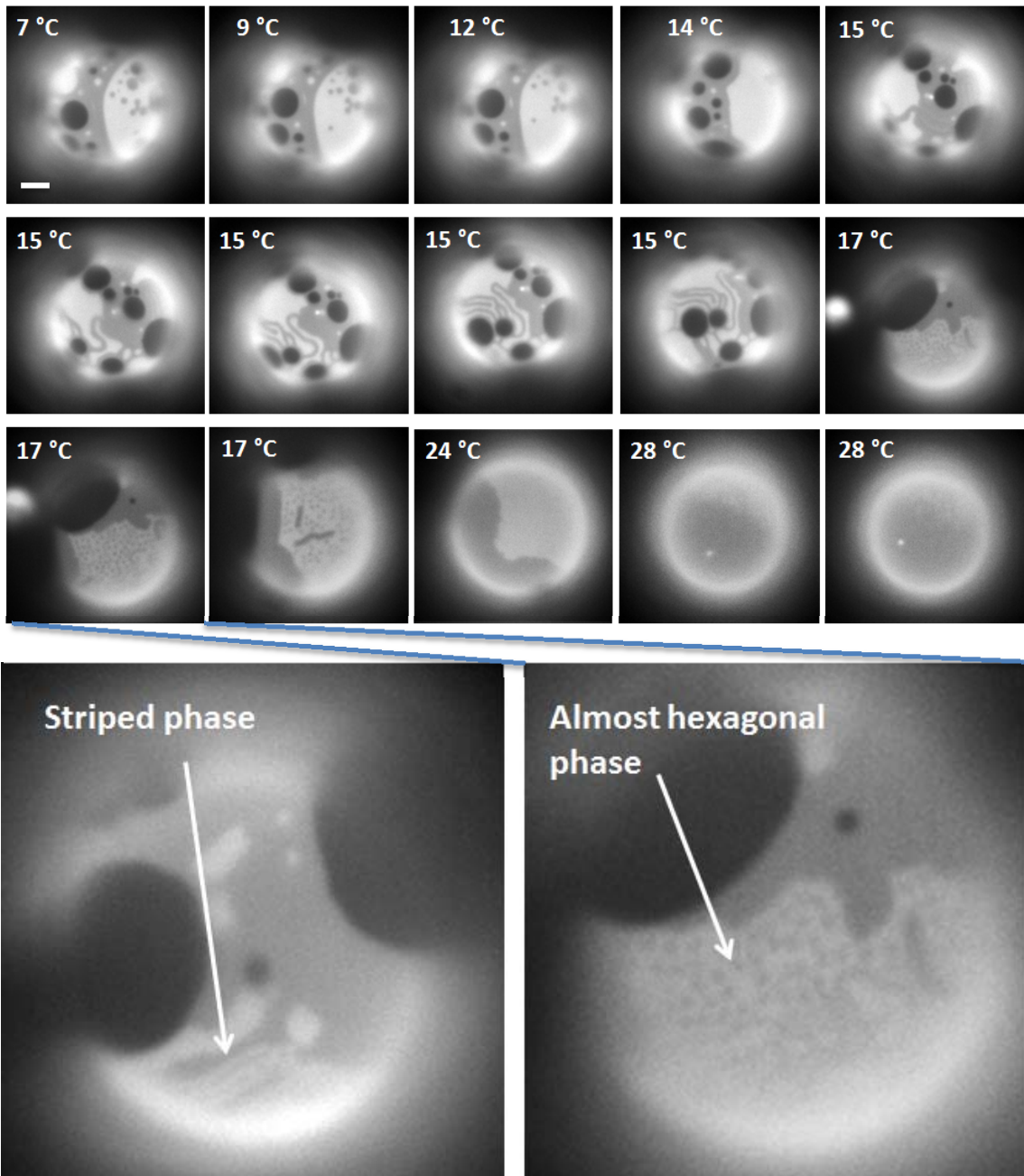


Fig. S20: Example of the appearance of striped domains upon temperature increase for a DiPhyPC/(24:1)SM/chol 1/1/1 + 1% Texas Red DHPE GUV. The striped domains appear after the decrease of the line tension between the domains with the highest fluorescence intensity and the domains with the intermediate intensity. Scale bar for the upper images = 10 μ m.

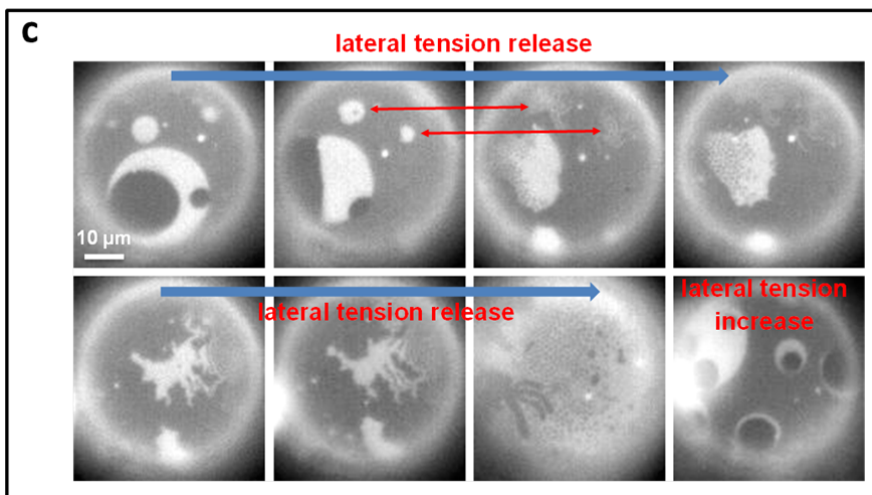
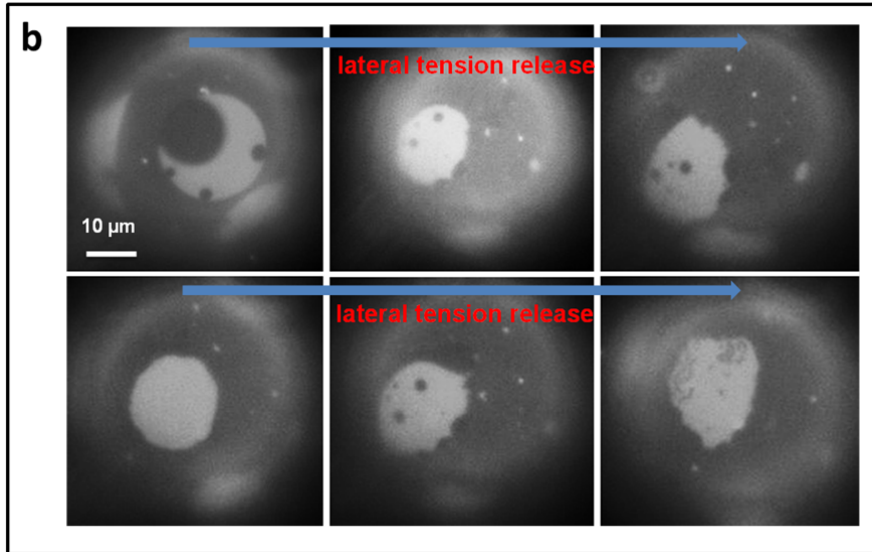
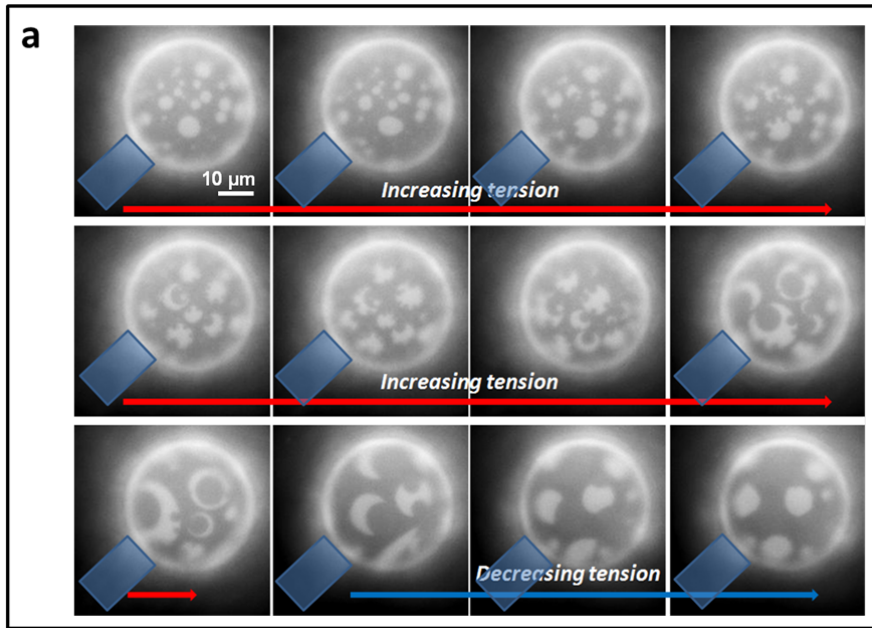


Fig. S21: a,b,c) Examples of shape changes of domains for DiPhyPC/(24:1)SM/Chol 1/1/1 (+ 1% Texas Red DHPE) GUVs upon an increase or release of the lateral tension obtained by a Micropipette Aspiration set-up at 15°C. The blue object in a) represents the position of the micropipette.

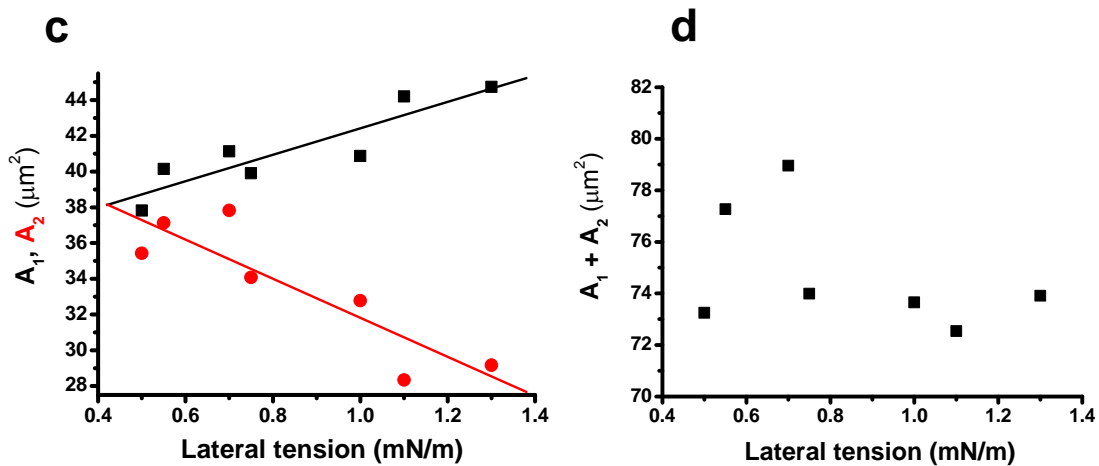
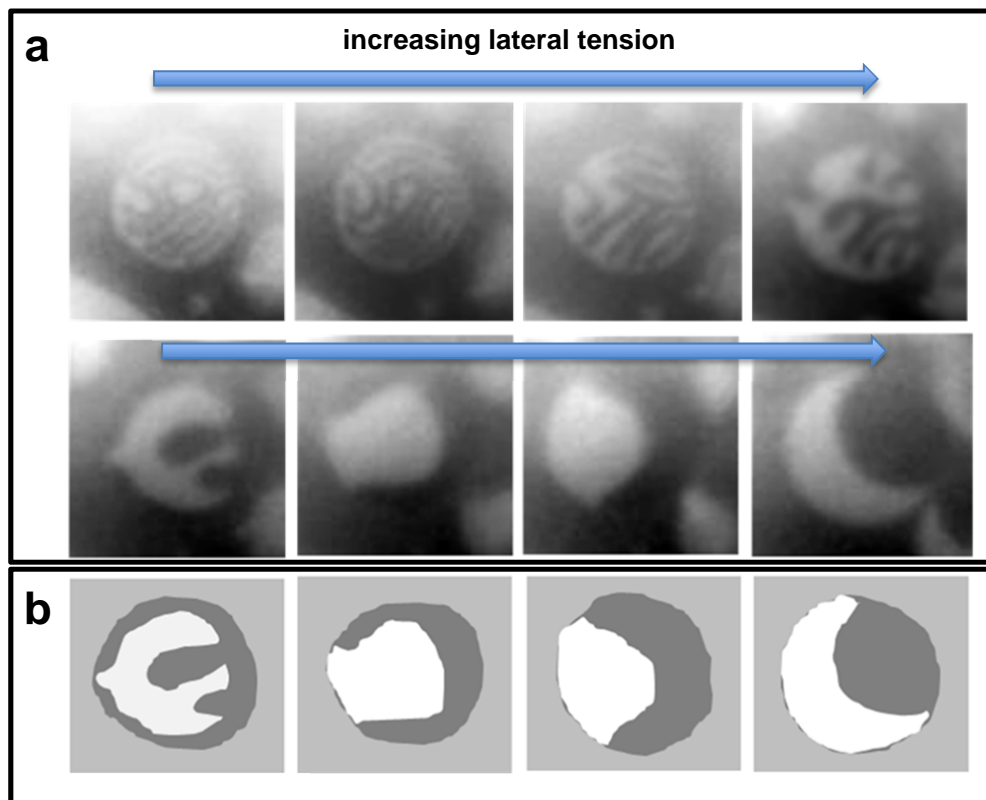


Fig. S22: a) Sequence of fluorescence microscopy images showing the detailed analysis of a domain in Fig. 10. b) Schematic representation of the domains corresponding to the second row in a); c) Quantitative analysis of the white (black squares) and dark grey (red dots) regions as a function of the applied lateral tension; d) Sum of the dark grey and white regions as a function of the applied lateral tension.

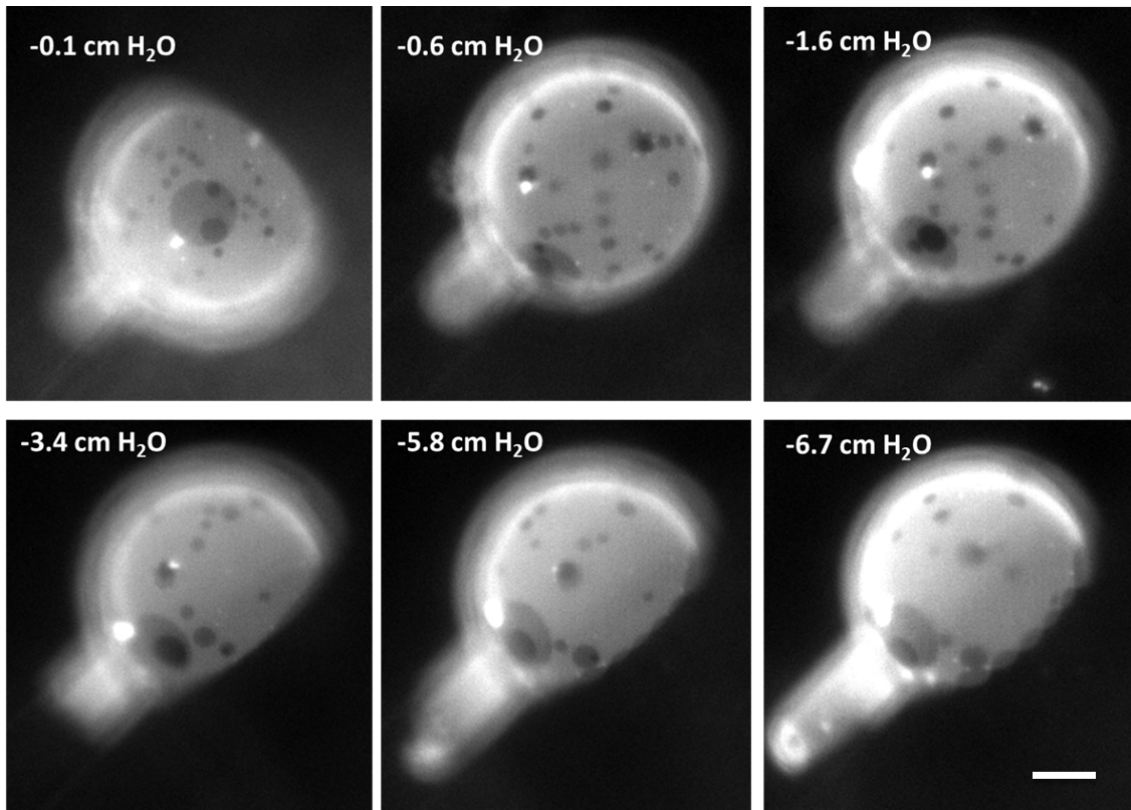


Fig. S23: Effect of the lateral tension on the shape of domains for a DiPhyPC/(24:1)SM/Chol 1/1/1 (+1% Texas Red DHPE) in the case of Type II domains of Fig. 5. Upon a lateral tension increase little effect is observed on the shape of the domains. Bar = 10 μm .

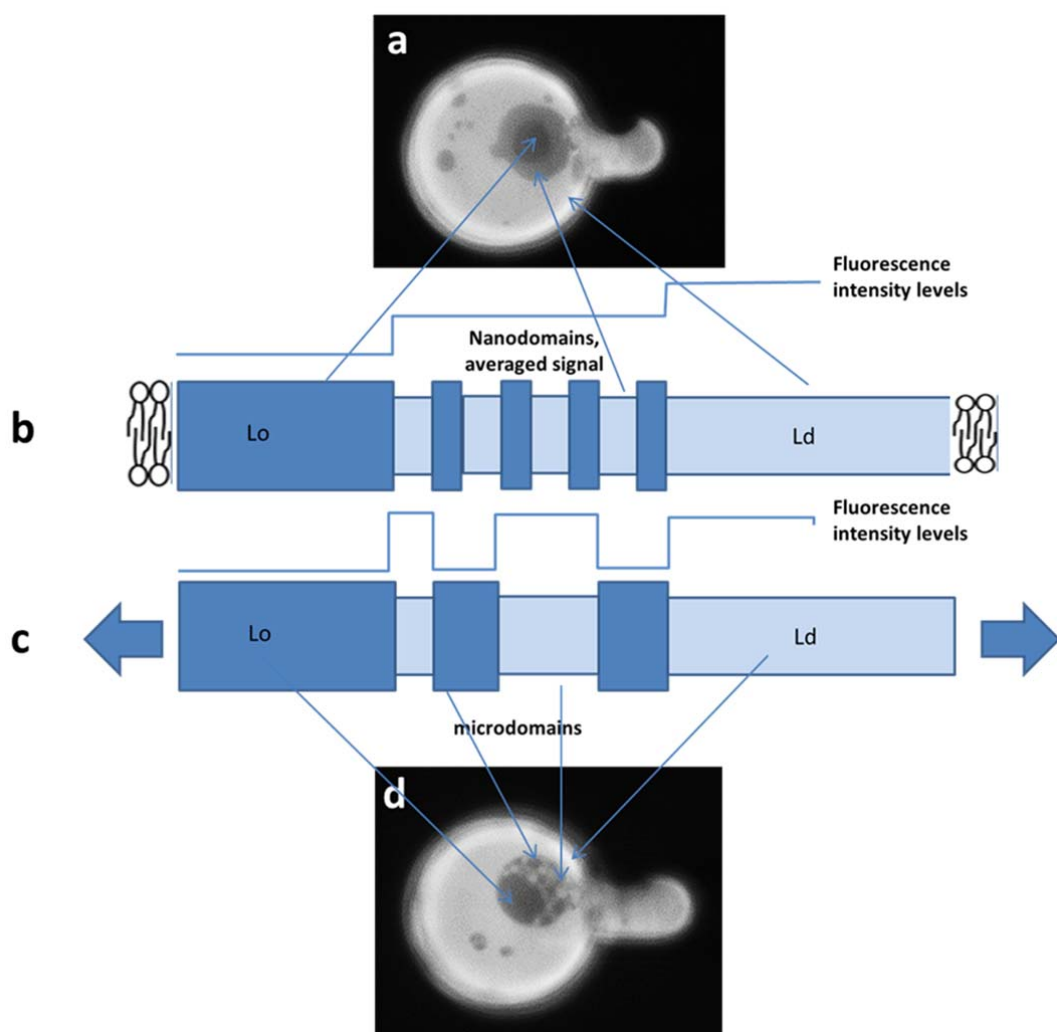


Fig. S24: Scheme of a possible interpretation for the appearance of the intermediate fluorescence intensity level upon temperature decrease and of its removal in favor of black (the darkest fluorescence level) and white (the highest fluorescence level) regions upon an increase of the lateral tension.

Line tension measurement

Theory

The line tension can be estimated from the (Fast) Fourier analysis of the L_o and L_d domains' contour fluctuations. The method is illustrated in detail in refs. [1], [2] but we provide here a brief account.

Given a selected domain, its image is recorded in time with a sufficient number of frames; for each frame, the radius as a function of the angle, $r(\vartheta)$, is extracted and the associated n -mode amplitudes $|u_n|$ are derived either by direct analysis or from the autocorrelation function $c(\delta) = \langle r(\vartheta)r(\vartheta+\delta) \rangle_{\vartheta} = (R_0^2/2)\sum_n |u_n|^2 \cos(n\delta)$, being R_0 the radius of a circle with the same area of the analyzed domain. The averages of the square amplitudes yield the line tension σ through [1]

$$\sigma = \frac{k_B T}{\pi R_0 (n^2 - 1) \langle |u_n|^2 \rangle},$$

where $k_B T$ is the thermal energy.

A 40x objective lens has been used, and the pixel size approximately corresponds to 114 nm. The exposure times range from 20 to 30 ms and the cycle times from 30 to 50 ms (if we increase the cycle time up to 250 ms the obtained results are very similar). Being the number of images for each sequence in the order of 600, the overall acquisition time takes 18-30 s. The domains are selected following the criteria indicated in [1,2], namely:

- Their area must not exceed 1/5 of the total area of a GUV
- Their shape must be almost circular
- Their radius must be not less than 3 μm
- They must be planar and located at about the center of the GUV imaged surface
- Their area must remain constant during the whole acquisition time

Selection of GUVs with appropriate domains is performed using as low as possible light intensity to prevent photo-oxidation. The images are collected by fluorescence microscopy; then, discrete approximations of the domain contours are obtained by superposing a square mesh mask to the images, which are converted to binary afterwards (the ImageJ software was used).

The length $\Delta x_{lim} = 114$ nm corresponding to the pixel size, poses a limit on the maximum mode number n_{max} which makes sense to be analyzed: the wavelengths of the Fourier components (e.g. in the autocorrelation function) are 2^n submultiples of the fundamental wavelength $\lambda_1 \equiv 2\pi R_0$, so that it is readily found that $n_{max} = \log_2(\lambda_1/\Delta x_{lim})$. Contours of domains with approximately 3 μm radius can be analyzed up to the 6th mode.

The problem of photo-oxidation has been considered already in ref. [2] and it is addressed here because we used a fluorophore concentration significantly higher (~ 5 times) than in that work. To check the relevance of induced photo-oxidation on the domains, we partitioned the image sequence in four sub-sets made of the same number of frames. For each sub-set the line tension was estimated in order to reveal whether any systematic drift of σ in time was detectable; our results did

not show any such tendency. Eventually, we analyzed the dependence of the line tension as a function of domain radius and, within errors, no influence on the domain size was observed.

Results

We compared the value of the line tension in the case of domains for a well-known lipid mixture (DiPhyPC/DPPC/Chol) with the case of domains of Type I (see manuscript) for the DiPhyPC/(24:1) SM/Chol mixture which showed the maximum sensitivity to the applied lateral tension. Fig. S24 shows typical examples of the domains we analyzed.

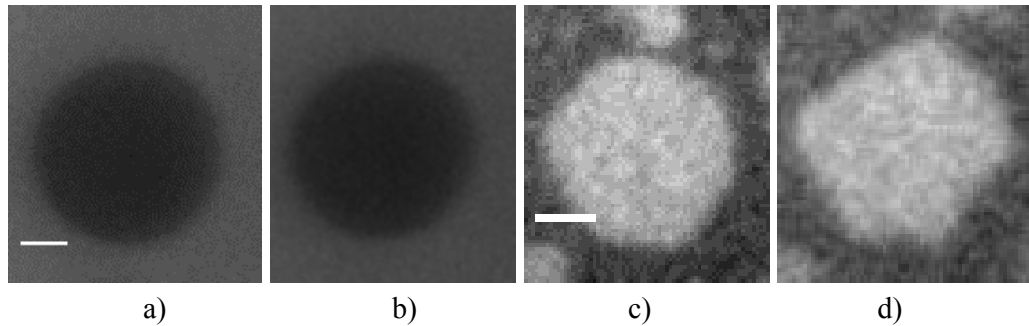


Fig. S25: a) and b) represent a L_o domain obtained from the DiPhyPC/DPPC/Chol mixture (1/1/1 molar ratio), as it appears in the initial and final frame of the analysis respectively. c) and d) represent a L_d domain obtained from the DiPhyPC/(24:1) SM/Chol mixture (1/1/1 molar ratio), as it appears in the initial and final frame respectively. Bar = 2 μm

Line tension components (Variance and mean amplitude):

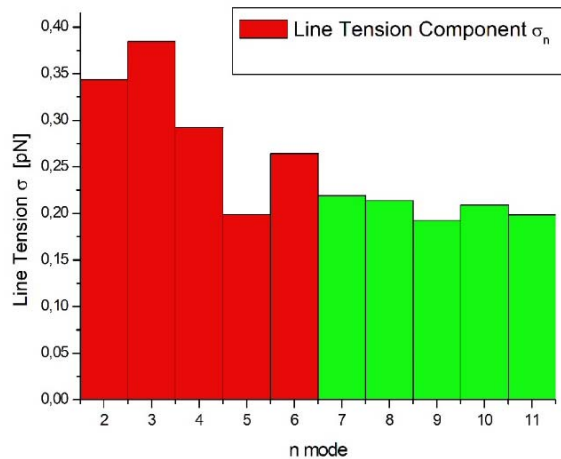


Fig. S26: Example of line tension estimate from different Fourier mode amplitudes as a function of mode number n . Only the first terms (up to the 6th mode) are relevant (red bars).

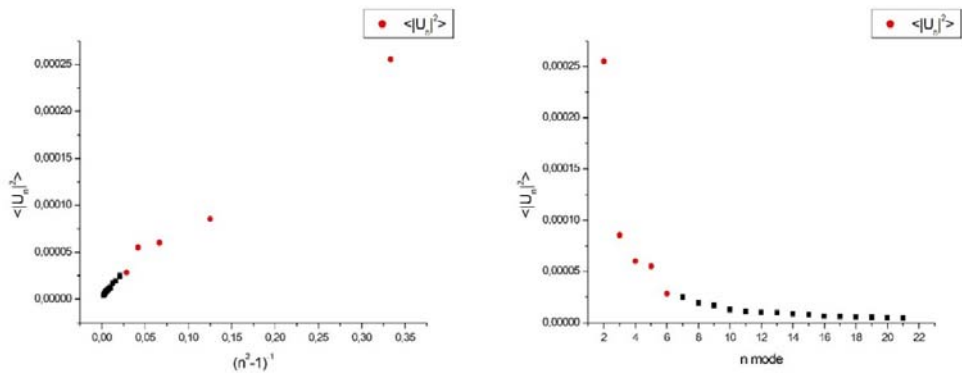


Fig. S27: Mean square amplitudes $\langle |u_n|^2 \rangle$ of the autocorrelation function as functions of $(n^2 - 1)^{-1}$ (left) and mode number n (right). Amplitudes from the 2nd to the 6th mode are plotted as red dots.

Line tension subsets

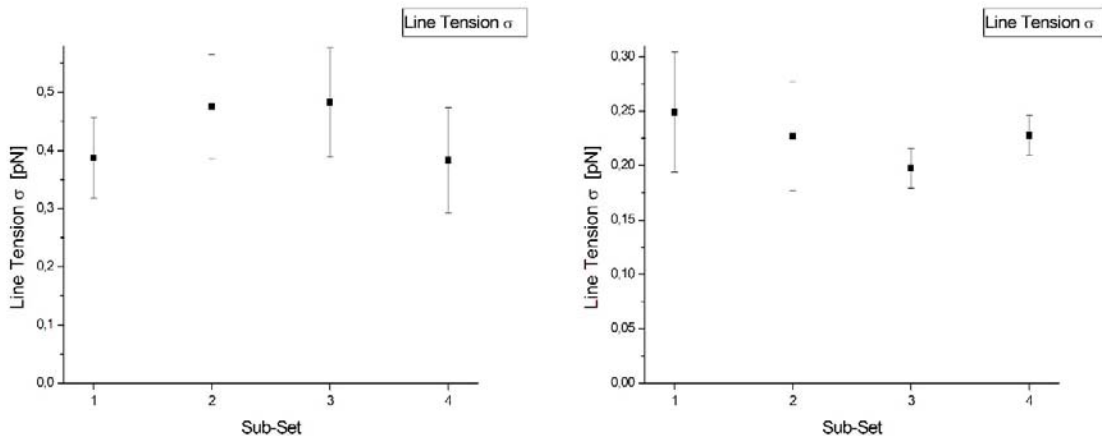
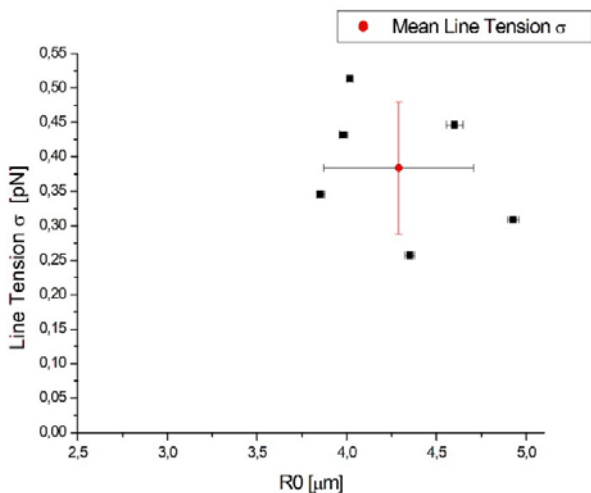


Fig. S28: Examples of estimated line tension for progressive sub-set number. The results do not show a significant dependence on the sub-sets; thus, the photo-oxidation process should be minimal.



Line tension as a function of domain radius

Fig. S29: Line tension as a function of domain radius for six L_o domains of a DiphyPC/DPPC/Chol 1/1/1 mixture. Only the domains with radius larger than 3 μm have been considered, as they allow to access a larger number of modes (up to the 6th one at least).

Line tension comparison

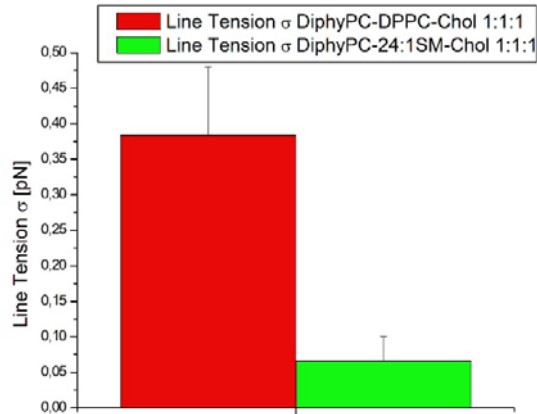


Fig. S30: Comparison of line tension estimates from L_o domains of DiPhyPC/DPPC/Chol 1/1/1 mixture (red) and L_d domains of DiPhyPC/(24:1) SM/Chol 1/1/1 mixture (green): The line tension for the domains in the first type of mixture (0.384 ± 0.096 pN) is larger than in the case of the second mixture (0.066 ± 0.035 pN).

References

- [1] Esposito C, Tian A, Melamed S, Johnson C, Tee SY, Baumgart T., Flicker spectroscopy of thermal lipid bilayer domain boundary fluctuations. *Biophys J.* 2007 Nov 1;93(9):3169-81
- [2] Usery RD, Enoki TA, Wickramasinghe SP, Weiner MD, Tsai WC, Kim MB, Wang S, Torng TL, Ackerman DG, Heberle FA, Katsaras J, Feigenson GW., Line Tension Controls Liquid-Disordered + Liquid-Ordered Domain Size Transition in Lipid Bilayers. *Biophys J.* 2017 Apr 11;112(7):1431-1443.

Movies' legends

Movie S1: Fluorescence microscopy movie of a DiPhyPC/bSM/Chol 1/1/1 (plus 1% Texas Red DHPE) vesicle undergoing a decreasing temperature ramp. The vesicle is grabbed by a micropipette (on the right of the vesicle, not visible in the fluorescence microscopy image). The temperature decreases from 50°C to 12°C. (see Figure 2 in the manuscript for other details).

Movie S2: Fluorescence microscopy movie of a DiPhyPC/bSM/Chol 1/1/1 (plus 1% Texas Red DHPE) vesicle showing the presence of three fluorescence intensity levels and undergoing an increase of the lateral tension at a constant temperature of 15°C. (See Figure 3 in the manuscript for other details).

Movie S3: Fluorescence microscopy movie of a DiPhyPC/(24:1)SM/Chol 1/1/1 (plus 1% Texas Red DHPE) vesicle at 15°C undergoing repetitive cycles of lateral tension increase and decrease. The lateral tension is increased by a micropipette aspiration set-up (the micropipette, not visible in the image, is positioned on the left of the vesicle at 45° with respect to the horizontal direction). (see Figure 10 in the manuscript for other details).

Movie S4: Another example of the same type of vesicle as in Movie S2. The vesicle undergoes a sequence of lateral tension increase and decrease. See Figure S20a for other details.

Movie S5: Another example of the same type of vesicle as in Movie S2. The vesicle undergoes a rapid lateral tension decrease. See Figure S20b for other details.